

# TeV gamma-ray observations of shell-type supernova remnants by the CAT telescope (2000-2001)

**B. Khélifi for the CAT Collaboration**

Physique Corpusculaire et Cosmologie, Collège de France et Université Paris VII, France (IN2P3/CNRS)

**Abstract.** The recent evidence of TeV  $\gamma$ -ray emission from the Supernova Remnant (SNR) Cassiopeia A (Aharonian *et al.*, 2001) demonstrates the interesting nature of these sources as candidate accelerators of cosmic rays. The observed TeV  $\gamma$ -ray emission may be produced by high-energy electrons and/or nuclei accelerated by shock fronts within the SNR. Here we report on observations by the CAT imaging Cherenkov telescope on the SNRs CTA 1 and IC443 during the years 2000–01. We also present our observations of the plerion CTB 80 during the same period. Gamma-ray flux upper limits are given for positions coincident with EGRET detections of each source.

---

## 1 Introduction

TeV  $\gamma$ -rays may be used to probe acceleration and propagation in the interstellar medium (ISM) of cosmic-rays (CR); CRs can produce  $\gamma$ -rays via bremsstrahlung and Inverse Compton (IC) processes from electrons and via nucleus-induced  $\pi^0$  decay. As SNRs are suspected of being possible sites of CR acceleration, numerous observations have been made in the TeV energy range (see Fegan *et al.*, 2001, for a recent review). The detection of the shell-type SNRs SN1006 (Tanimori *et al.*, 1998), RXJ 1713.7-3946 (Muraishi *et al.*, 2000) and Cassiopeia A have been claimed at these energies. We have selected the Shell-type SNRs CTA 1 and IC443 based on criteria including distance and age, on energy spectral slope in the GeV range and on the angular size of the error box of the EGRET detection, as well as the presence of molecular clouds. These parameters are summarised in Table 1. Some authors (e.g., Brazier *et al.*, 1998) suggest that the remnant CTA 1 contains a pulsar (not detected yet). Also, CTB 80 contains the 39.5 ms pulsar PSR 1951 + 32.

## 2 The CAT telescope and data analysis

The CAT (Cherenkov Array at Thémis) imaging atmosphere Cherenkov telescope (Barrau *et al.*, 1998) is located on the site of the former solar plant at Thémis in the French Pyrénées (2° East, 42° North, altitude 1650 m above sea level). The Cherenkov light emitted by cosmic-ray showers is collected by a 17.8m<sup>2</sup> Davies-Cotton mirror and detected by a very high definition camera, which is composed by 546 phototubes with 0.12° angular diameter in a 3.1° field of view, surrounded by larger phototubes in two guard rings extending the field of view to 4.8°. The fast trigger electronics located in the camera allow us to reach a detection threshold (defined as the energy at which the differential  $\gamma$ -ray rate is maximum at the trigger level for a Crab-like source) as low as 250 GeV at Zenith. This very high definition allows an efficient rejection of the huge cosmic-ray background by means of an accurate analysis based on the comparison of individual images with theoretical mean  $\gamma$ -ray images (Le Bohec *et al.*, 1998). A  $\chi^2$  fit to a mean light distribution predicted from electromagnetic showers simultaneously provides the likelihood level of a  $\gamma$ -ray origin and, if this hypothesis is correct, a measurement of the  $\gamma$ -ray energy with an accuracy (RMS) of 22%. This fitting procedure gives an estimation of the source position for each shower with an accuracy of the order of pixel size. The localization accuracy for a bright point source is 1'.

For the study of these galactic sources, we suppose that the  $\gamma$ -ray emission comes from a *point* source. Indeed, we suppose that the emission of CTB 80 comes from the pulsar PSR 1951 + 32, which is not resolved by our detector. For the CTA 1 remnant, we observed the EGRET position, which is close to the centre of the brightest region of diffuse emission in X-rays from the source. Slane *et al.* (1997) and Brazier *et al.* (1998) suggest that a pulsar is situated at this position. The size of EGRET error box for the SNR IC443 (see Table 1) is smaller than our PMT size.

The system of data analysis, which allows an efficient discrimination between  $\gamma$ -rays and CR background, is described

Source	l deg.	b deg.	RA hhmmss	DEC ddmmss	Dist Kpc	Age Ky	Presence of molecular clouds	EGRET $\times 10^{-7} \text{ cm}^{-2} \text{ s}^{-1}$	Diff. Index	Error box $\theta_{95\%}$ (deg.)
CTA 1	119.5	10.2	001014	731700	1.4	5	no	$46.4 \pm 6.2$	$-1.58 \pm 0.18$	0.24
IC 443	189.3	3.2	061800	223400	1.5 - 2.0	4 - 13	yes	$50 \pm 4$	$-2.01 \pm 0.06$	0.13
CTB 80	69.0	2.7	195258	325240	3	10	–	$6.0 \pm 1.4^a$	$-1.74 \pm 0.11$	–

**Table 1.** Summary of some parameters for CAT galactic targets. We give the integrated flux of EGRET above 100 MeV and the differential index of a power law spectrum.

<sup>a</sup> The EGRET flux for CTB 80 is the pulsed component from PSR1951 + 32.

in detail in Piron *et al.* (2001). In order to search for weak point sources (compared to the Crab nebula flux), our cuts have been optimized using a Monte Carlo simulated signal of  $0.5\gamma$  per minute (before cuts) superimposed on a real background. We require that the total charge in the image be greater than 52 photo-electrons (p.e.). However the shape cut remains at the same value as the standard cut with a  $\chi^2$  probability greater than 0.35. As we have supposed that the sources’ size is smaller than the pixel size, the  $\gamma$ -ray image points towards the source angular position in the focal plane. As the CR directions are isotropic, we use the cut  $\alpha < 5^\circ$ , where the pointing angle  $\alpha$  is defined as the angle at the image barycentre between the supposed source angular position and the source position reconstructed by the fit. These cuts reject  $\sim 99.9\%$  of hadronic events while keeping  $\sim 28\%$  of  $\gamma$ -ray events. The hadronic background surviving the preceding cuts is monitored by comparing ON and OFF-source observations at the same telescope elevation. The OFF are normalized using a tracking ratio defined by the ratio  $n_{\text{ON}}/n_{\text{OFF}}$  of the number of events surviving the shape cuts in the region  $20^\circ \leq \alpha \leq 120^\circ$ .

### 3 Data sample and results

The observations were performed between July 2000 and February 2001. The range in zenith angles of the CTB 80 sample extends from close to the Zenith to  $35^\circ$ , for CTA 1 from  $30^\circ$  to  $40^\circ$  and for IC443 from  $20^\circ$  to  $30^\circ$ . ON-source runs last for  $\sim 30$  minutes followed or preceded by OFF-source runs shifted by  $\pm 35'$  in right ascension from the source position. For CTB 80, the observations have been taken with the source  $S$  shifted  $0.29^\circ$  away from the center  $O$  of the field of view. The showers pointing towards the symmetrical position with respect to  $O$  have been used to monitor the background and considered as OFF-source data. This procedure allows increased ON-source observation time as OFF-source data are not taken, but disallows a study of extended sources. These samples are selected for clear weather conditions and stable detector operation. The pointing positions, the numbers of observation hours and the results of “ON-OFF” analyses are summarised in the Table 2 for the three sources after run selection. The data were analysed separately by zenith angle region to take account of variations in efficiency; the results are combined in this table.

We note that no signal is recorded for these galactic sour-

ces. We derived upper limits of flux level with a confidence interval level of 99.73% (i.e.,  $3\sigma$ ) for each source. The calculation of the flux upper limits is based on an interval estimation for a classical statistic (Eadie *et al.*, 1971). The derived integral flux above our threshold, 250 GeV, used an effective area (which is a function of the zenith angle, see Piron *et al.*, 2001) using a spectral shape of the hypothetical source parametrized by a power law with a differential index either of  $-2.80$  or of  $-2.40$ . The results are presented in Table 3. The pointing positions are those from Table 2.

	Differential index -2.80	Differential index -2.40
CTA 1	$4.15 \times 10^{-11}$	$2.64 \times 10^{-11}$
IC 443	$2.15 \times 10^{-11}$	$1.54 \times 10^{-11}$
CTB 80	$3.79 \times 10^{-11}$	$2.82 \times 10^{-11}$

**Table 3.** Upper limits on integral fluxes above 250 GeV for the 99.73% confidence level, for two differential indices of a power law shape. The unit of the integral fluxes is  $\text{cm}^{-2} \text{ s}^{-1}$ .

### 4 Discussion

We summarise all the observations in Figure 1. We note that CAT upper limits for CTA 1 are below the extrapolation from the EGRET integral data points. This could suggest a steepening of the  $\gamma$ -ray spectrum and/or a spectral break between the VHE upper limits and the EGRET energy range.

CTA 1  $\gamma$ -ray emission is still not understood. The models of the power source responsible for high-energy emission may be either an acceleration process between the SNR shock on the local ISM (via Fermi acceleration) or a pulsar wind. The relatively low ISM density at the observed position ( $\sim 1 \text{ cm}^{-3}$ ) and the EGRET hard spectrum could favour the latter suggestion. However, no pulsed emission has been detected from this SNR. A more constrained VHE limit and/or observations at other wavelengths (e.g., in radio, in the GeV/-100 GeV  $\gamma$ -ray range) could clarify the physical process of acceleration in CTA 1.

According to Gaisser *et al.* (1998), who simulated interactions between SNR and ISM, the  $\gamma$ -ray emission from IC443 could largely result from IC and bremsstrahlung radiation. It can be seen that the CAT upper limit is below the predicted level from this model, which is fitted to the EGRET data. However, the model does not take into account the presence

Source	RA deg	DEC deg	T <sub>ON</sub> hours	T <sub>OFF</sub> hours	N <sub>ON</sub> events	N <sub>OFF</sub> events	Tracking ratio	Excess events	Standard deviation events	significance n <sub>σ</sub>
CTA 1	2.5685	73.1742	9.9	7.4	945	676	1.40	14.4	48.1	0.30
IC 443	94.5126	22.5663	13.7	9.9	1133	909	1.28	-13.6	53.2	-0.25
CTB 80	298.2420	32.8779	10.4	10.4	1013	953	1.00	59.4	44.4	1.34

**Table 2.** Analysis results for each target. RA and DEC refer to the pointing positions of the telescope.

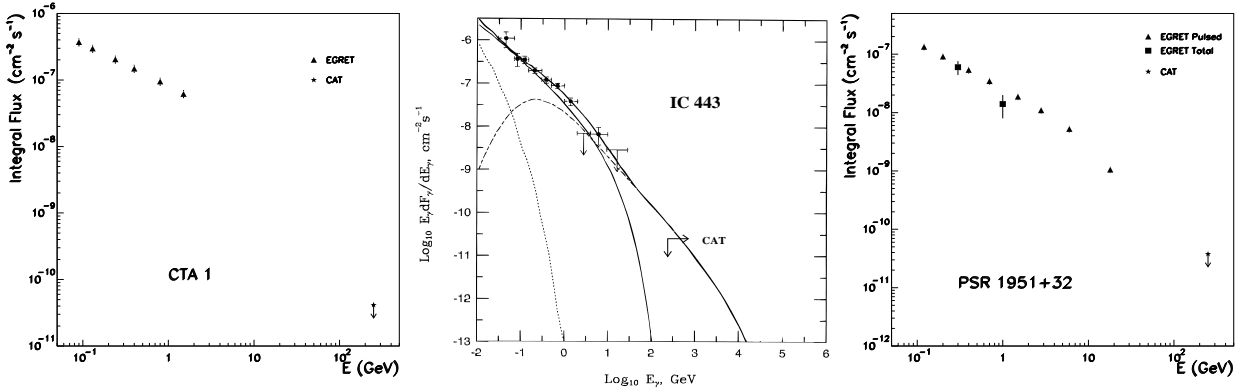


**Fig. 1.** Compilation of EGRET data and 99.73% upper limits of this work for a differential index value of  $-2.8$ . The EGRET results are taken from Brazier *et al.* (1998) and from Ramanamurthy *et al.* (1995). The different curves are from Gaisser's model. The dashed curve is IC on the microwave background, the dotted curve is  $\pi^0$  production, the lower solid curve is Bremsstrahlung and the upper solid curve is the total emission.

of molecular clouds (see CO maps from Cornett *et al.*, 1977). Their presence would greatly enhance the local ISM density, and would lower the predicted flux at VHE energies. They would, however, give a spectrum in contradiction with the EGRET data.

The observations of the SNR CTB 80 are taken at the position of the pulsar PSR 1951 + 32. Our result could constrain the  $\gamma$ -ray emission both from the pulsar and the plerionic shell (e.g., the emission region, matter density, . . . ).

## 5 Conclusion

The CAT imaging Cherenkov telescope observed an SNR, a plerion and an SNR with plerion characteristics over the period 2000–01. We report the point source flux upper limits for IC443, CTB 80 and for CTA 1 (table 2). These limits are derived with a power law spectrum for a hypothetical source with a differential index value of  $-2.80$  and  $-2.40$ . These limits could constrain the VHE  $\gamma$ -ray emission of the sources, indicating a possible spectral break between the EGRET energy range and the VHE range. However, these limits suffer from a lack of observation time, as the period of 2000–01 was marked by very poor weather conditions in the Pyrénées. Further observations are ongoing. Other types of analysis are under development in order to obtain more constrained upper limits over our full field of view.

## References

- Aharonian, F. A., *et al.* 2001, A&A 370, 112
- Barrau, A., *et al.* 1998, NIM A416, 278
- Brazier, K. T. S., *et al.* 1998, MNRAS, 295, 819
- Cornett, R. H., *et al.* 1977, A. Ap. 54, 889
- Eadie, W. T., *et al.* 1971, Statistical methods in experimental physics, Ed. North-Holland
- Fegan, S., *et al.* 2001, astro-ph/0102324
- Gaisser, T. K., *et al.* 1998, ApJ, 492, 219
- Le Bohec, S., *et al.* 1998, NIM A416, 425
- Li, T. P., Ma, Y. Q., 1983, ApJ, 272, 317L
- Muraishi, H., *et al.* 2000, ApJ, 537, 422
- Piron, F., *et al.* 2001, A&A to be published
- Ramanamurthy, P. V., *et al.* 1995, ApJ, 447, L109
- Slane, P., *et al.* 1997, ApJ, 485, 221
- Tanimori, T., *et al.* 1998, ApJ, 492, L33